ELSEVIER

Biochemical Pharmacology 63 (2002) 1251–1258

Biochemical Pharmacology

Induction of G_2/M arrest and inhibition of *c-myc* and *p53* transcription by WP631 in Jurkat T lymphocytes

Silvia Villamarín[a], Neus Ferrer-Miralles[a], Sylvia Mansilla[a], Waldemar Priebe[b], José Portugal[a,*]

[a]*Departamento de Biología Molecular y Celular, Instituto de Biología Molecular de Barcelona, CSIC, Jordi Girona 18-26, 08034 Barcelona, Spain*
[b]*Department of Bioimmunotherapy, M.D. Anderson Cancer Center, The University of Texas, Houston, TX 77030, USA*

Received 23 May 2001; accepted 11 December 2001

Abstract

WP631, a new DNA-binding drug that bisintercalates into DNA with high affinity, seems to be highly cytotoxic against Jurkat T lymphocytes. The purpose of this study was to gain new insights into the mechanisms by which WP631 halts proliferation in this cell type. Treating Jurkat cells with nanomolar concentrations of WP631 produced G_2/M arrest, inhibited the transcription of *c-myc* and *p53* genes, and induced limited apoptosis during the duration of treatment. Suppression of *c-myc* and *p53* expression, and time-dependent decline in c-Myc and p53 protein levels, was associated with growth arrest. A weak interdependence was also found between the potent antiproliferative activity and the apoptotic response; treatment with WP631 for 24–36 hr produced arrest in G_2/M and allowed for partial DNA repair. Longer treatments with WP631 allowed some repaired cells to re-enter the cell cycle, but produced aneuploidy or apoptosis in others.

Keywords: DNA binding; G_2 phase; Jurkat cells; *c-myc*; *p53*; Polyploidy

1. Introduction

Small molecules that bind with high affinity to DNA and recognize extended sequences are being explored as potential antitumor agents [1–4]. Recent studies on targeting small molecules to specific sequences in DNA have led to the design of novel DNA-binding bisintercalating agents with significantly increased DNA-binding affinity [2,5] and high antitumor activity. One such molecule, WP631 (Fig. 1), was designed on the basis on the structure of DNA–daunorubicin complexes [2]. WP631 shows an ultratight binding affinity for a six base-pair DNA sequence, which is of the same range of several DNA-binding proteins [2,4,6,7]. At nanomolar concentrations, WP631 displaces the Sp1 transcription factor from its binding site in promoters, thereby interfering strongly with the eukaryotic transcription machinery *in vitro* [8]. This is accompanied by a remarkable biological activity. Preliminary studies have established that WP631 is more active than some monoanthracyclines against the breast carcinoma MCF-7/VP-16 cell line, in which it overcomes a specific form of multidrug resistance [2]. It is also more potent than daunorubicin or doxorubicin in inhibiting the growth of Jurkat T lymphocytes [9].

In the present study, we explored the mechanisms that account for the cytotoxicity of WP631. Jurkat cells treated with nanomolar concentrations of WP631 showed accumulation in the G_2/M phase and limited apoptotic death over a 72 hr interval. Since susceptibility to drug-induced apoptosis in leukemia cells seems to be regulated by *c-myc* and *p53*, among other genes [10], the levels of their mRNAs and proteins were also analyzed to study the possible relationship between WP631, the expression of these genes and cell growth arrest.

2. Materials and methods

2.1. Cell line and culture conditions

Jurkat T lymphocytes were obtained from the cell culture facilities at the Department of Biochemistry of the University of Barcelona, Spain. Cells were maintained in RPMI

* Corresponding author. Tel.: +34-93-400-61-76; fax: +34-93-204-59-04.
E-mail address: jpmbmc@cid.csic.es (J. Portugal).

Abbreviations: MTT, 3-(4,5-dimethylthiazol-2-yl)-2,5-diphenyltetrazolium bromide; *GAPDH*, glyceraldehyde-3-phosphate dehydrogenase.

0006-2952/02/$ – see front matter
PII: S0006-2952(02)00865-1

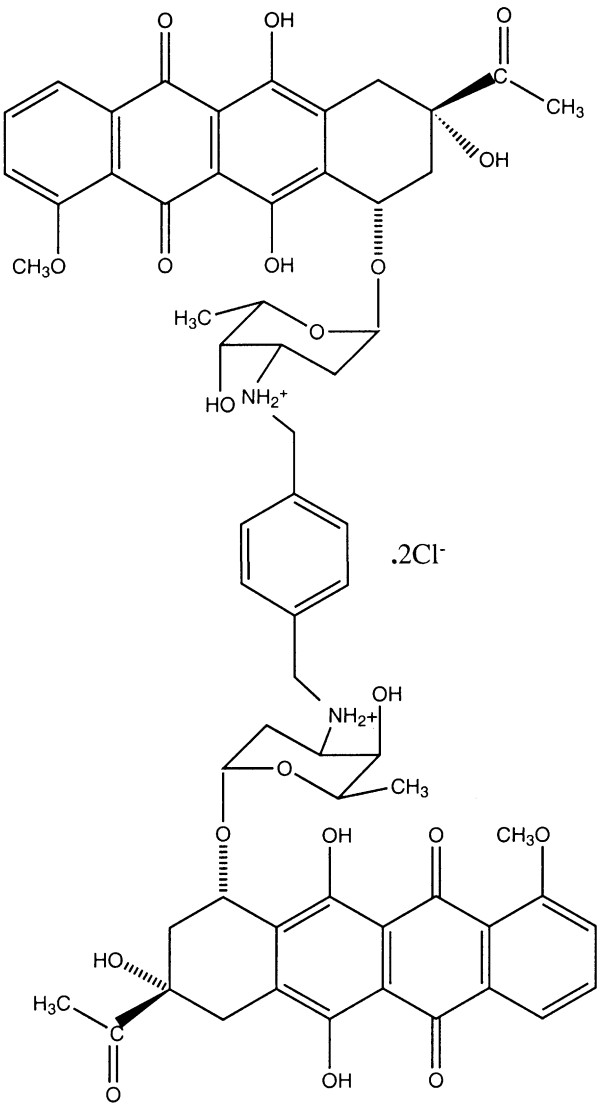

Fig. 1. Chemical structure of WP631.

1640 medium (GibcoBRL); supplemented with 10% fetal calf serum (GibcoBRL) and 2 mM L-glutamine (GibcoBRL), at 37° in a humidified atmosphere with 5% CO_2.

A 500 μM stock solution of WP631 was prepared with sterile 150 mM NaCl, maintained −20°, and brought to the final concentration with RPMI 1640 medium just before use.

2.2. Growth arrest and cell death assays

The capacity of WP631 to interfere with the growth of Jurkat cells was determined by the 3-(4,5-dimethylthiazol-2-yl)-2,5-diphenyltetrazolium bromide (MTT) dye assay [11] in 96-well microtiter plates (Coming Costar) with flat-bottomed wells, in a total volume of 100 μL. Cells subcultured at a density of 5×10^4 cells/mL were incubated with various concentrations of WP631 at 37° for 72 hr. Upon completion of the incubation, MTT (Sigma) was added to each culture (15 μL per well). The dark-colored crystals that were produced by viable cells were solubilized with 30 mM HCl in 2-propanol. Absorbance was determined at 570 nm using a SPECTRAmax-250 microplate spectrofluorometer (Molecular Devices). Viable cell number was determined based on the exclusion of Trypan Blue (Fluka) as described elsewhere [12].

2.3. Morphological examination

The morphology of Jurkat cells after drug treatment was analyzed by light microscopy. Smears were prepared by spreading a cell suspension with the edge of a coverslip. The smears were air-dried, stained with 20% Wright-Giemsa and coverslipped. Apoptotic cells were identified by the presence of cytoplasmic shrinking and nuclear condensation.

2.4. Flow cytometry

After treatment with WP631 for various periods, the cells were harvested and stained with propidium iodide (Sigma) as described elsewhere [13]. Nuclei were analyzed with an Epics Elite flow cytometer (Coulter Corporation) at the 'Serveis Cientifico-Tecnics de la Universitat de Barcelona,' using the 488 nm line of an argon laser and standard optical emission filters. Cell percentages at each phase of the cell cycle were estimated from their DNA content histograms after drug treatment. Apoptosis was quantified and distinguished from necrosis by using the Annexin-V-Fluos staining kit (Roche Diagnostics) and flow cytometry in accordance with described procedures [14] using 488 nm excitation and 515 nm bandpass filter for fluorescence detection.

2.5. Analysis of internucleosomal DNA damage

Qualitative analysis of DNA fragments resulting from internucleosomal cleavage in cells undergoing apoptosis was carried out by following procedures described elsewhere [15], with minor modifications. Briefly, 2×10^6 Jurkat T cells treated with WP631—or with daunorubicin (Sigma) for comparison—were lysed in 40 μL of a buffer consisting of 10 mM Tris–HCl (pH 7.4), 10 mM NaCl, 1 mM EDTA, 0.5% SDS and 0.5 mg/mL proteinase K for 1 hr at 50°. Thereafter, 1 μL of 1 mg/mL RNAse A was added and incubated for 2 hr at 50°. The high molecular weight DNA was precipitated by addition of NaCl up to 1 M. After centrifugation, at 500 *g* for 30 min, the supernatants were collected by ethanol precipitation and the pellets resuspended in 50% glycerol containing 0.02% bromophenol blue. Samples were analyzed by electrophoresis in 1.8% agarose gels, stained with 0.5 μg/mL ethidium bromide, and photographed under UV light.

2.6. Northern blot analysis

Total RNA was isolated from WP631-treated and control cells (those to which no drug was added) by using the

UltraspecRNA isolation reagent (Biotecx) according to the procedure provided by the vendor. RNA samples were denatured in 0.02 M 3-(*N*-morpholino)propanesulfonic acid (pH 7.0) containing 2.2 M formaldehyde and 50% formamide, and transferred to a Hybond-N+ membrane (Amersham Biosciences). Radiolabeled probes for human *c-myc* exon 2, *p53* (kindly provided by Evelyne May) and *GAPDH* c-DNA were prepared by using Ready-to-Go Labeling Beads (Amersham Biosciences) and [α-^{32}P]dCTP. The blots were hybridized with the labeled probes and washed under stringent conditions before autoradiography [16]. Signal intensities were quantified in a Molecular Dynamics densitometer and normalized using the *GAPDH* probe as reference.

2.7. Western blot analysis

Protein was extracted from WP631-treated and control cells, at the indicated times, with a lysis buffer consisting of 50 mM Tris–HCl (pH 8), 150 mM NaCl, 5 mM EDTA, 0.5% Nonidet P-40, 0.1 mM phenilmethylsulphonil fluoride, containing protease inhibitors. Total protein was quantified by the Bradford assay (Bio-Rad). Denatured proteins (30–50 μg per sample) were subjected to electrophoresis on SDS-polyacrylamide gels (12% for c-Myc and p53 and 10% for actin), blotted onto Optitran BA-S85 membranes (Schleicher & Schuell), analyzed with antibodies (purchased from Sigma and Oncogene), and detected by chemiluminescence using luminol (Sigma). Signal intensities were quantified in a Molecular Dynamics densitometer and normalized using actin as reference.

3. Results

Over the course of a 72 hr drug treatment, WP631 produced a concentration-dependent decrease in cell growth. Its IC_{50} (drug concentration required to inhibit cell growth by 50%), determined from dose–response curves, was 18 nM, and its IC_{75} (drug concentration required to inhibit cell growth by 75%) was 60 nM, in agreement with our previous findings with Jurkat cells [9]. We thus aimed to gain new insights into the mechanisms followed by WP631 to halt cell proliferation.

Morphological changes observed after that Jurkat cells were exposed to 60 nM WP631 for 72 hr (Fig. 2) included chromatin condensation and nuclear fragmentation corresponding to apoptotic cells. Although these effects were pronounced, they affected only a limited number of cells (Fig. 2A).

Cells treated with WP631 were also analyzed by flow cytometry and double staining with propidium iodide and Annexin-V-fluorescein (Fig. 3) to distinguish necrotic cells (propidium iodide staining) from the translocation of phosphatidylserine to the outer layer of the plasma membrane (Annexin-V) [14]. The total amount of apoptotic plus necrotic cells was rather small, especially in light of the low WP631 concentration required to stop cell growth. They represented, through the total period of treatment, about 5–10% of cells. The number of apoptotic cells was between 4% at 24 hr (Fig. 3B) and around 8% at 72 hr. Continuous exposure to WP631 did not produce a significant change in the number of cells suffering necrosis or apoptosis, compared to the control. However, after 72 hr treatment the double staining (propidium iodide plus Annexin-V) uncovered the presence of an additional 2% of apoptotic cells, which were not evident by using the less sensitive flow cytometry analysis with propidium iodide staining only.

Ethidium bromide-stained agarose gels (Fig. 4) showed internucleosomal DNA fragmentation, a hallmark of apoptosis, in cells treated with WP631 or daunorubicin. Therefore, from a qualitative point of view, WP631 did induce some apoptotic cell death in Jurkat cells. However, the results presented in Fig. 3 suggest that apoptosis was infrequent in the total population of quiescent cells after WP631 treatment.

Flow cytometry was used to evaluate the effect of WP631 on the cell cycle distribution. In the absence of WP631 (Fig. 5A), the average distribution of the lymphocytes corresponded to 37.1% G_0/G_1, 28.3% S phase, and 33.5% G_2/M, with a 1.1% sub-G_1 peak. After 32 hr of drug treatment (Fig. 5B) the distribution was 29.7% G_0/G_1, 17.7% S phase, and 42.6% G_2/M, with a 10% sub-G_1 peak. These values are similar to those previously obtained at 36 hr [9]. The effects of treatment with WP631 for up to 36 hr on G_2 accumulation are shown in Fig. 6A. Thereafter, the proportion of cells in G_2 became similar to that of the

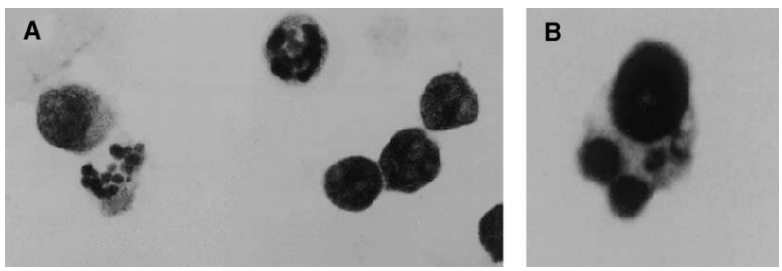

Fig. 2. Effect of WP631 on the morphology of Jurkat T lymphocytes. (A) A 20% Wright-Giemsa stained preparation. Morphological changes include condensation of chromatin, nuclear fragmentation, membrane blabbing, and formation of apoptotic bodies; (B) a magnified cell (2.5×) showing details of the apoptotic bodies after 72 hr treatment with 60 nM WP631 (IC_{75}).

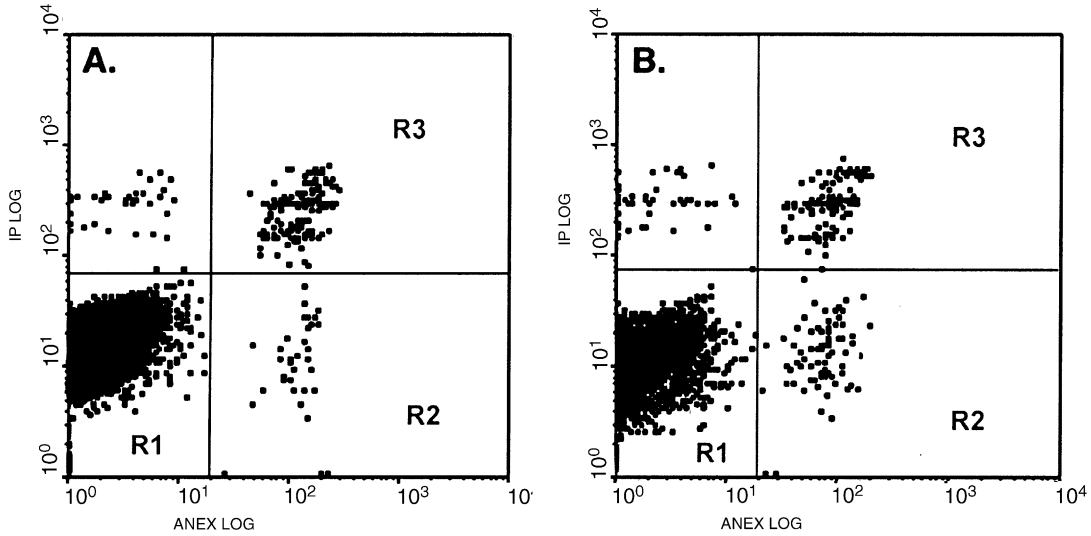

Fig. 3. Flow cytometry analysis of apoptotic Jurkat cells stained with Annexin-V-Fluos and propidium iodide. (A) Control untreated cells; (B) cells treated with 60 nM WP631 for 24 hr. Quadrant R1 living cells, R2 apoptotic cells, R3 necrotic cells. Apoptotic cells are characterized by high Annexin-V-Fluos staining and low propidium iodide staining.

untreated control cells. Fig. 6B shows the influence of WP631 on the viability of Jurkat cells, measured by Trypan Blue exclusion, at different times, together with the analysis of cell proliferation using MTT assays, which measures the antiproliferative effect of WP631 (i.e. cells which are not metabolically active). These experiments showed that the IC_{75} of WP631 produced low growth inhibition over 32–36 hr treatment, followed by a decline in the number of proliferating cells (empty bars in Fig. 6B) reaching a 25% at 72 hr. However, the same time-dependent proportion number of non-viable Trypan-stained cells did no decrease much (filled bars in Fig. 6B). Treatment with WP631 for 62–72 hr-induced polyploidy (Fig. 7) whereas untreated Jurkat cells maintained a nearly uniform distribution of cells in each phase of the cell cycle. The number of apoptotic and necrotic cells at 72 hr could not be quantified in this experiment directly. In fact, apoptotic G_2-phase cells exhibit a reduced DNA content, which could overlap the content of G_1-cells. Nevertheless, they were calculated as about 12% by double staining with propidium iodide and Annexin-V-fluorescein.

We treated exponentially growing Jurkat cells with WP631 and analyzed the expression of the oncogene *c-myc* because the c-Myc protein targets genes are involved in cell growth, apoptosis, and in arrest at both the G_1 and G_2 checkpoints [17,18]. We also analyzed the transcription of the *p53* gene, because the p53 protein is essential in the apoptotic response to many drugs [19], and mediates apoptosis by preventing the proliferation induced by oncogene activation [20]. Northern blot analyses (Fig. 8)

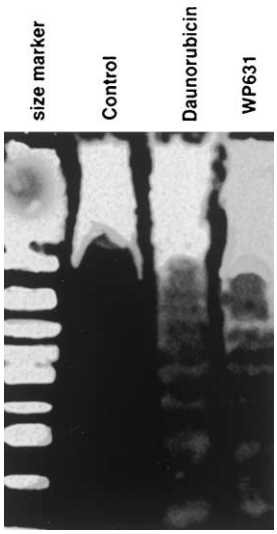

Fig. 4. Agarose gel analysis of the apoptosis-associated internucleosomal DNA fragmentation in Jurkat cells treated with 60 nM WP631 for 18 hr. The effect of daunorubicin is shown for comparison.

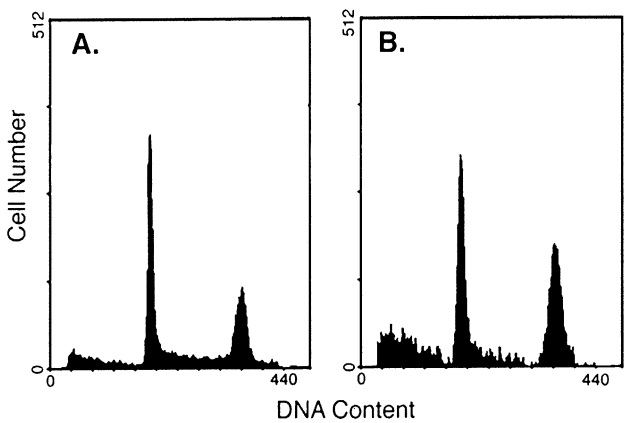

Fig. 5. Cell cycle distribution of Jurkat T cells in the absence (A) and the presence of 60 nM WP631 for 32 hr (B), analyzed by propidium iodide staining and flow cytometry. Increases in sub-G_1 and G_2/M peaks are evident after treatment.

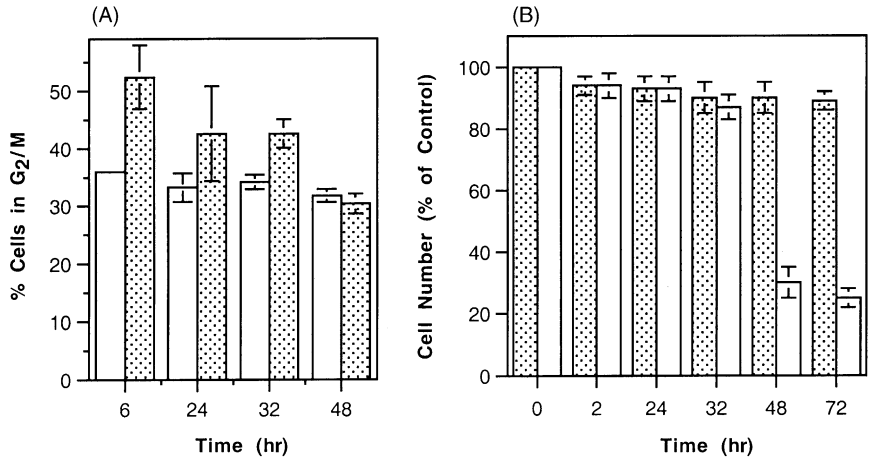

Fig. 6. (A) Percentage of Jurkat cells arrested in the G_2/M phase of the cell cycle after WP631 treatment (empty bars) control, untreated cells; (filled bars) cells treated with 60 nM WP631, for the times in the figure. Data are means ± SD for three-four independent experiments. Accumulation in G_2 was statistically significant at 6, 24 and 32 hr of treatment ($P < 0.05$, Student's *t*-test). (B) A comparative plot of the influence of 60 nM WP631 (IC_{75}) on the time-dependent "cell growth inhibition" (six replicate MTT assays) (empty bars), and "number of viable cells" (filled bars) (three replicate Trypan Blue experiments). Data presented are the means ± SEM.

showed that the exposure of Jurkat T lymphocytes to WP631 produced a time-dependent decrease in both *c-myc* and *p53* mRNA levels by about 80% after 3 hr of treatment (Fig. 8B), whereas the expression of the housekeeping *GAPDH* remained almost unaltered. Reduction in *c-myc* and *p53* RNA levels can prevent apoptosis [20]. The inhibition of *p53* mRNA synthesis may also influence G_1/S and G_2/M checkpoints [21,22] and participate in the appearance of aneuploidy (Fig. 7 and [23]).

Fig. 9 shows the time-dependent reduction on the levels of the *c-myc* and *p53* proteins in the presence of WP631. After about 4 hr of continuous treatment with the bisanthracycline, both protein levels decreased in parallel, although, after 24 hr, the amount of c-Myc was clearly lower than p53 (Fig. 9B). The presence of some c-Myc protein during the first hours of treatment may be required to abate G_1 arrest, allowing cells to go to phase S. The rapid decrease in p53 after about 32 hr (slope of the curve in Fig. 9B), and the concomitant materialization of polyploidy, would indicate that p53 played an important role in maintaining the G_2 arrest shown in Fig. 6A. These results agree with p53 involvement in G_2 arrest [24].

The experiments presented in Figs. 8 and 9 strongly suggest that Jurkat T cells, which were in a transient G_2-arrest after treatment with WP631 (Fig. 6A), might

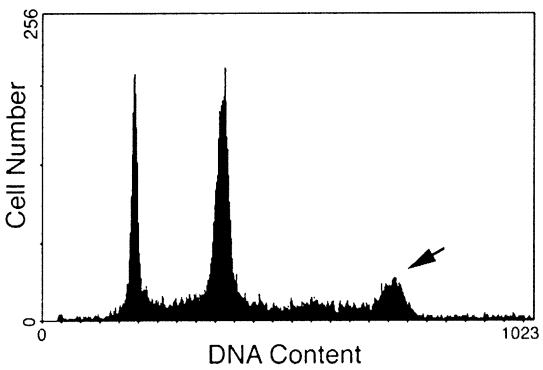

Fig. 7. Flow cytometry analysis of Jurkat T cells in the presence of 60 nM WP631, after 62 hr of continuous treatment. A peak corresponding to aneuploid cells is indicated by the arrow.

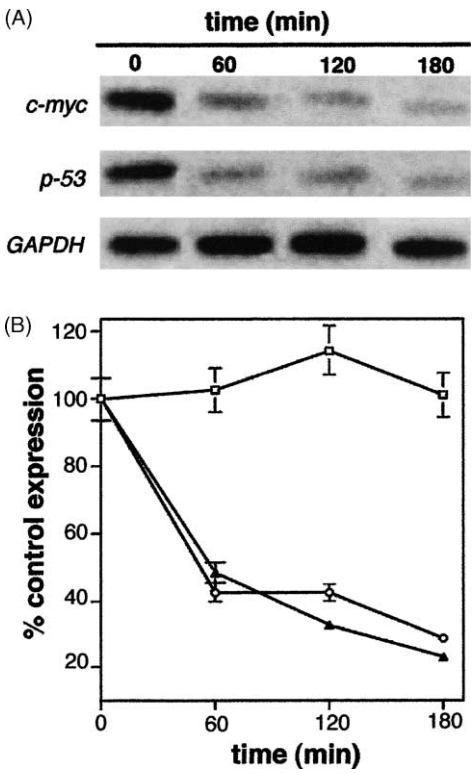

Fig. 8. (A) A representative Northern blot showing time-dependent reduction in *c-myc* and *p53* expression, but not in the housekeeping *GAPDH* gene exposed to 60 nM WP631 (IC_{75}). (B) Quantitative representation of the time-dependent suppression of gene expression by WP631 in Jurkat cells: *c-myc* (▲), *p53* (○) and *GAPDH* (□). Data are the means ± SD for three experiments, normalized for *GAPDH* expression.

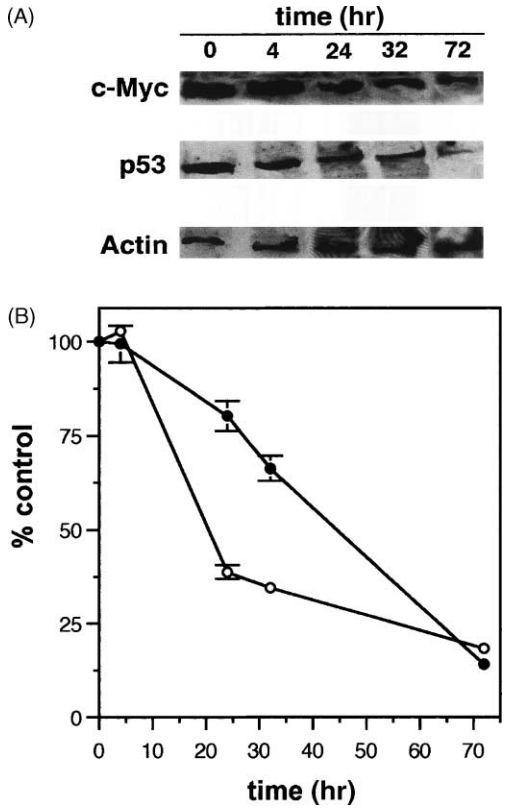

Fig. 9. (A) A representative Western blot showing time-dependent reduction in c-Myc and p53 levels, but not in the actin levels, in Jurkat T cells exposed to 60 nM WP631. (B) Quantitative representation of the time-dependent decrease in protein levels by WP631, as percent of protein at time 0. c-Myc (○), p53 (●). Data are the means ± SD for two independent experiments, normalized for the levels of actin.

overcome the G_2 checkpoint when p53 levels clearly decreased after about 32 hr. This resulted in polyploidy (Fig. 5), with only about 5% death cells, but 75% of quiescent cells measured using the MTT proliferation assay (Fig. 6B).

4. Discussion

Strong transcription inhibitors like WP631 [8,9] can induce quiescence in growing Jurkat cells at rather low concentrations and can inhibit the transcription of several genes such as *p53* and *c-myc*, which are associated with cellular proliferation and are also important in apoptosis.

WP631 is a strong growth inhibitor of some tumor cells in culture [2,9]. The apparent cell growth inhibition in our study, measured by MTT assay, resulted from several factors. Not all Jurkat T cells underwent apoptosis after treatment with WP631 over a 62 hr period, but rather underwent either immediate or delayed growth cessation, which was accompanied by an increase in the DNA content per cell. The cytotoxic effects of WP631 in Jurkat cells could be accompanied by other additional events like DNA damage, which is frequently linked to G_2/M arrest [12,25]. Damage in DNA might be enhanced through the collision between trapped topoisomerase II cleavage complexes and the replication fork, or transcription complexes [26]. Some cell death should appear if cells with unrepaired damage attempt mitosis, thus explaining the marginal presence of apoptotic cells (Fig. 3). The accumulation of Jurkat cells in G_2 until about 36 hr treatment (Fig. 6) might also be connected with the capacity of p53 to maintain growth arrest in G_2.

We observed the presence of aneuploid cell changes that occurred during still longer treatments. Notably, daunorubicin causes higher apoptotic cell death in Jurkat T cells in similar experimental conditions [27]. G_2 arrest is considered an effect of DNA-binding agents because cells engaged in cell division are particularly susceptible to DNA damage [15,28,29]. This arrest would demand p53 activity [29]. Protein levels decreased in a time-dependent manner, and, after about 32–36 hr (Fig. 9), the cells that elicited G_2 block without fully restored DNA integrity would result in the observed polyploidy (Fig. 7). In the present study, we report a time-dependent decrease in p53 protein, which was followed by polyploidy at longer periods of treatment. A result that agrees with the correlation that has been established between loss of *p53* and genetic instability [30]. These findings are consistent with other reports that low levels of p53 render cells more susceptible to gene amplification and the development of aneuploidy [23,31]. Prolonging the G_2/M transition would permit some cells to repair DNA and complete their replication [32]. Our results substantiate that several cytostatic drugs perturb the cell cycle distribution and produce changes in DNA content, which lead to a remarkable increase in cell mass and ploidy [29,30].

Reduced *c-myc* expression occurs in response to drugs that produce mainly G_2 arrest, but it is the inhibition of *p53* gene that mainly determines the extent of growth arrest and apoptosis [21,22]. WP631 clearly decreased the levels of *p53* mRNA. The decrease in the levels of c-Myc protein after treatment with WP631 possibly affected the G_1 checkpoint, a result that is in keeping with the low apoptosis detected (Fig. 3). Jurkat cells failed to arrest in G_1. The absence of G_1 arrest in Jurkat cells, despite the inhibition of *c-myc* transcription after 2–4 hr treatment, can be explained by the presence of previously synthesized c-Myc protein (cf Figs. 8 and 9). Notwithstanding, the absence of G_1 arrest can also be due to other defects in checkpoint function, as it has been described in other cell lines in the presence of certain drugs [33].

The refractoriness of MCF-7 cells to apoptosis induced by doxorubicin [12,34] or WP631 [9] and the limited apoptosis observed in Jurkat T cells after 72 hr treatment agrees with finding that the transcription of *c-myc* was highly sensitive to nanomolar concentrations of WP631 (Fig. 8). There is a known association between the effects of some drugs on *c-myc* expression and the response to DNA damage in MCF-7 cells [12,34]. We recently reported

a diminution in *c-myc* RNA levels, without apoptosis, in MCF-7 cells as a result of WP631 treatment [9]. However, internucleosomal DNA fragmentation was observed in Jurkat cells (Fig. 4). Since the synthesis of *p53* mRNA was also strongly inhibited by WP631 in a time-dependent manner, the limited apoptosis in Jurkat cells during the first 12–24 hr of treatment could have resulted from storage of the protein in the cytoplasm, as detected by Western blot analysis (Fig. 9), or through a different mechanism independent of p53. Hence, WP631 should directly produce cell cycle arrest in G_2 (quantified in Fig. 6). An effect that may be enhanced by the indirect effect of p53 on the down-regulation of *c-myc*. The presence of limited apoptosis during the 72 hr of continuous exposure to the drug is not at variance with the presence of active p53-independent apoptotic pathways in Jurkat cells [35].

In summary, we have found an apparent interdependence between the low *c-myc* and *p53* RNA levels observed after drug treatment, the time-dependent decrease in c-Myc and p53, and cell cycle arrest. From a quantitative point of view, the main effect of WP631 on Jurkat T lymphocytes is cell arrest at the G_2 checkpoint, at least during the first 36–48 hr of treatment, which was followed by polyploidy. These results support, but do not prove, that in Jurkat T lymphocytes, altered *c-myc* expression by WP631 is directly linked to cell pathways leading to growth arrest. A similar correlation has been described for DNA-binding agents in other cell lines [9,34,36]. Transcription inhibition seems to be more complex in a cell system than *in vitro*, in which WP631 was a strong inhibitor in basal and Sp1-activated transcription [8]. Since the human *c-myc* contains a Sp1-responsible promoter ([37], and references therein) cell distribution in the different phases of the cell cycle may be associated with the extend of transcription of the oncogene. Nevertheless, a WP631 effect on the binding of Sp1 to the *c-myc* promoter *in vivo* does not imply specificity, since *p53* was also inhibited, even though it lacks functional Sp1-binding sites in the proximal promoter [38]. Nevertheless, the inhibition of p53 transcription could be an indirect consequence of the absence of the c-Myc trans-activation of the *p53* promoter [39]. Additional genes may be altered *in vivo*. The use of DNA arrays, together with the determination of the levels of different proteins other than p53 and c-Myc, should provide us with further evidences about the genes ultimately responsible of the antiproliferative effects of WP631. Experiments along these aspects are being undertaken in our laboratory.

Acknowledgments

This work was financed by grants from the Spanish DGESIC (PB96-0812 and PB98-0469), The Welch Foundation and the Commission for Scientific Exchange between the United States of America and Spain. The support of the Centre de Referencia en Biotecnologia is also acknowledged.

References

[1] Lown JW. Design of sequence-specific agents: lexitropsins. In: Neidle S, Waring M, editors. Molecular aspects of anticancer drug–DNA interactions, vol. 1. London: MacMillan, 1993. pp. 322–55.
[2] Chaires JB, Leng FF, Przewloka T, Fokt I, Ling YH, Perez-Soler R, Priebe W. Structure-based design of a new bisintercalating anthracycline antibiotic. J Med Chem 1997;40:261–6.
[3] Gottesfeld JM, Neely L, Trauger JW, Baird EE, Dervan PB. Regulation of gene expression by small molecules. Nature 1997; 387:202–5.
[4] Leng F, Priebe W, Chaires JB. Ultratight DNA binding of a new bisintercalating anthracycline antibiotic. Biochemistry 1998;37: 1743–53.
[5] Priebe W, editor. Antracycline antibiotics: new analogues, methods of delivery and mechanisms of action. In: Proceedings of the ACS Symposium Series. Washington (DC): American Chemical Society, 1995.
[6] Hu GG, Shui X, Leng F, Priebe W, Chaires JB, Williams LD. Structure of a DNA–bisdaunomycin complex. Biochemistry 1997;36:5940–6.
[7] Robinson H, Priebe W, Chaires JB, Wang AHJ. Binding of two novel bisdaunorubicins to DNA studied by NMR spectroscopy. Biochemistry 1997;36:8663–70.
[8] Martín B, Vaquero A, Priebe W, Portugal J. Bisanthracycline WP631 inhibits basal and Sp1-activated transcription initiation *in vitro*. Nucleic Acids Res 1999;27:3402–9.
[9] Portugal J, Martín B, Vaquero A, Ferrer N, Villamarín S, Priebe W. Analysis of the effects of daunorubicin and WP631 on transcription. Curr Med Chem 2001;8:1–8.
[10] Lotem J, Sachs L. Control of apoptosis in hematopoiesis and leukemia by cytokines, tumor suppressor and oncogenes. Leukemia 1996;10:925–31.
[11] Mosmann T. Rapid colorimetric assay for cellular growth and survival: application to proliferation and cytotoxicity assays. J Immunol Meth 1983;65:55–63.
[12] Fornari FA, Jarvis WD, Grant S, Orr MS, Randolph JK, White FKH, Gewirtz DA. Growth arrest non-apoptotic cell death associated with the suppression of *c-myc* expression in MCF-7 breast tumor cells following acute exposure to doxorubicin. Biochem Pharmacol 1996; 51:931–40.
[13] Doyle A, Griffiths JB, Newell DG. Cell and tissue culture: laboratory procedures. New York: Wiley, 1995.
[14] Vermes I, Haanen C, Steffens-Nakken H, Reutelingsperger C. A novel assay for apoptosis: flow cytometric detection of phosphatidylserine expression on early apoptotic cells using fluorescein-labelled Annexin V. J Immunol Meth 1995;184:39–51.
[15] Skladanowski A, Konopa J. Adriamycin and daunomycin induce programmed cell death (apoptosis) in tumour cells. Biochem Pharmacol 1993;46:375–82.
[16] Sambrook J, Fritsch EF, Maniatis T. Molecular cloning: a laboratory manual. New York: Cold Spring Harbour, 1989.
[17] Evan GI, Wyllie AH, Gilbert CS, Littlewood TD, Land H, Brooks M, Waters C, Penn LZ, Hancock DC. Induction of apoptosis in fibroblasts by c-Myc protein. Cell 1992;69:119–28.
[18] Dang CV. *c-myc* target genes involved in cell growth, apoptosis, and metabolism. Mol Cell Biol 1999;19:1–11.
[19] Lowe SW, Ruley HE, Jacks T, Housman DE. p53-dependent apoptosis modulates the cytotoxicity of anticancer agents. Cell 1993;74:957–67.
[20] Hermeking H, Eick D. Mediation of c-Myc-induced apoptosis by *p53*. Science 1994;265:2091–3.

[21] Enoch T, Norbury C. Cellular responses to DNA damage: cell cycle checkpoints, apoptosis and the roles of p53 and ATM. Trends Biochem Sci 1995;20:426–30.
[22] Chen X, Ko LJ, Jayaraman L, Prives C. p53 levels, functional domains, and DNA damage determine the extent of the apoptotic response of tumor cells. Genes Dev 1996;10:2438–51.
[23] Jacks T, Weinberg RA. Cell cycle control and its watchman. Nature 1996;381:643–4.
[24] Bunz F, Dutriaux A, Lengauer C, Waldman T, Zhou S, Brown JP, Sedivy JM, Kinzler KW, Vogeistein B. Requirement for p53 and p21 to sustain G_2 arrest after DNA damage. Science 1998;282:1497–501.
[25] Yu YQ, Giocanti N, Averbeck D, Megnin-Chanet F, Favaudon V. Radiation-induced arrest of cells in G_2 phase elicits hypersensitivity to DNA double-strand break inducers and an altered pattern of DNA cleavage upon re-irradiation. Int J Radiat Biol 2000;76:901–12.
[26] Fortune JM, Osheroff N. Topoisomerase II as a target for anticancer drugs: when enzymes stop being nice. Prog Nucleic Acid Res Mol Biol 2000;64:221–53.
[27] da Silva CP, de Oliveira CR, da Conceiçao M, de Lima P. Apoptosis as a mechanism of cell death induced by different chemotherapeutic drugs in human leukemic T lymphocytes. Biochem Pharmacol 1996;51:1331–40.
[28] Ling YH, Elnaggar AK, Priebe W, Perez-Soler R. Cell cycle-dependent cytotoxicity, G_2/M phase arrest, and disruption of p34(cdc2)/cyclin b-1 activity induced by doxorubicin in synchronized P388 cells. Mol Pharmacol 1996;49:832–41.
[29] Kaufmann WK, Kies PE. DNA signals for G_2 checkpoint response in diploid human fibroblasts. Mutat Res 1998;400:153–67.
[30] Purdie CA, Harrison DJ, Peter A, Dobbie L, White S, Howie SE, Salter DM, Bird CC, Wyllie AH, Hooper ML. Tumour incidence, spectrum and ploidy in mice with a large deletion in the *p53* gene. Oncogene 1994;9:603–9.
[31] Yin XY, Grove L, Datta NS, Long MW, Prochownik EV. c-Myc overexpression and p53 loss cooperate to promote genomic instability. Oncogene 1999;18:1177–84.
[32] Bedi A, Barber JP, Bedi GC, el-Deiry WS, Sidransky D, Vala MS, Akhtar AJ, Hilton J, Jones RJ. BCR-ABL-mediated inhibition of apoptosis with delay of G_2/M transition after DNA damage: a mechanism of resistance to multiple anticancer agents. Blood 1995;86:1148–58.
[33] Magnet KJ, Orr MS, Cleveland JL, Rodriguez-Galindo C, Yang H, Yang C, Di YM, Jain PT, Gewirtz DA. Suppression of *c-myc* expression and c-Myc function in response to sustained DNA damage in MCF-7 breast tumor cells. Biochem Pharmacol 2001;62:593–602.
[34] Bunch RT, Povirk LF, Orr MS, Randolph JK, Fornari FA, Gewirtz DA. Influence of amsacrine (m-AMSA) on bulk and gene-specific DNA damage and *c-myc* expression in MCF7 breast tumor cells. Biochem Pharmacol 1994;47(3):17–29.
[35] Vigorito E, Plaza S, Mir L, Mongay L, Viñas O, SerraPages C, Vives J. Contributions of p53 and PMA to gamma irradiation-induced apoptosis in Jurkat cells. Hematol Cell Ther 1999;41:153–61.
[36] Gewirtz DA, Randolph JK, Chawla J, Orr MS, Fornari FA. Induction of DNA damage, inhibition of DNA synthesis and suppression of *c-myc* expression by the anthracycline analog, idarubicin (4-demethoxy-daunorubicin) in the MCF7 breast tumor cell line. Cancer Chemother Pharmacol 1998;41:361–9.
[37] Vaquero A, Portugal J. Modulation of DNA–protein interactions in the P1 and P2 *c-myc* promoters by two intercalating drugs. Eur J Biochem 1998;251:435–42.
[38] Tuck SP, Crawford L. Characterization of the human *p53* gene promoter. Mol Cell Biol 1989;9(2):163–72.
[39] Reisman D, Elkind NB, Roy B, Beamon J, Rotter V. c-Myc transactivates the p53 promoter through a required downstream CACGTG motif. Cell Growth Differ 1993;4:57–65.